Electronic Supplementary Information (ESI)

Long wavelength NIR luminescence of 2,2'-bipyridyl-Pt(II) dimers achieved by enhanced Pt-Pt interaction

Meng-Meng Su, Jun Ni,* Zhong-Cui Guo, Shu-Qin Liu, Jian-Jun Zhang and Chang-Gong Meng

School of Chemical Engineering, Dalian University of Technology, Linggong Road No. 2, Dalian 116024, P. R. China

* Corresponding author.

E-mail: nijun@dlut.edu.cn

Contents

Table S1. Crystal data and structure refinement for complexes **1**, **2**, **5** and **6**.

	1	**2**	**5**	**6**
Empirical formula	$C_{44}H_{50}N_2PtSi_2$	$C_{46}H_{54}N_2PtSi_2$	$C_{42}H_{44}Cl_2N_2PtSi_2$	$C_{42}H_{44}Br_2N_2PtSi_2$
M	858.13	886.18	898.96	987.88
Crystal system	monoclinic	monoclinic	monoclinic	monoclinic
Space group	*C2/c*	*P2/c*	*C2/c*	*C2/c*
a / Å	41.9131(12)	21.9102(16)	42.451(4)	42.721(4)
b / Å	14.9174(4)	15.4983(13	14.8742(14)	15.0203(16)
c / Å	13.0806(4)	13.0730(9)	13.1745(12)	13.1674(14)
β / °	93.1230(10)	103.155(4)	95.890(3)	95.929(5)
V / Å^3	8166.3(4)	4322.7(6)	8274.8(13)	8404.1(15)
Z	8	4	8	8
D_c /g cm^{-3}	1.396	1.362	1.443	1.562
μ(mm^{-1})	3.526	3.333	3.609	5.328
Radiation (λ, Å)	0.71073	0.71073	0.71073	0.71073
T / K	210(2)	210(2)	200(2)	210(2)
F(000)	2712	1800	3600	3888
R_{int}	0.035	0.039	0.161	0.027
Reflections collected / uniques	16356/7089	14648/7557	71115/7279	18689/7293
Observed reflections ($I > 2\sigma(I)$)	5688	5425	4854	5758
$R1^a$($I > 2\sigma(I)$)	0.0405	0.0451	0.0549	0.1162
$wR2^b$(all data)	0.1157	0.01175	0.1453	0.2729
GOF	1.002	1.018	1.072	1.108

$^a R1 = \Sigma|F_o - F_c|/\Sigma F_o$, $^b wR2 = \Sigma[w(F_o^2 - F_c^2)^2]/\Sigma[w(F_o^2)]^{1/2}$.

Table S2. Selected bond lengths (Å) and angles (°) for complexes **1**, **2**, **5** and **6**.

	1	**2**	**5**	**6**
Pt–Pt (within dimer)	3.1737(4)	3.1674(4)	3.1973(7)	3.1925(8)
Pt–Pt (between dimers)	4.9276(3)	4.9813(4)	4.9139(5)	4.8767(7)
Pt–N	2.060(5)	2.052(6)	2.066(7)	2.130(10)
	2.062(6)	2.059(5)	2.067(8)	2.067(10)
Pt–C	1.932(7)	1.955(8)	1.923(10)	1.964(6)
	1.961(7)	1.972(10)	1.933(10)	1.954(4)
N1–Pt–N2	79.3(2)	78.8(2)	78.9(3)	78.5(4)
C–Pt–C	88.9(3)	88.9(3)	88.3(4)	89.4(4)
N1–Pt–C	96.5(2)	96.6(3)	97.4(3)	94.8(4)
	174.0(2)	173.9(2)	173.9(3)	175.7(4)
N2–Pt–C	95.4(3)	95.8(3)	95.4(3)	97.2(3)
	175.7(2)	175.3(3)	176.3(3)	172.9(4)

Table S3 Important hydrogen-bonding geometry (Å,°) and short interactions in **1**, **2**, **5**, and **6**.

		1			
D-H ··· *A*	*D*-H	H ··· *A*	*D* ··· *A*	*D*-H ··· *A*	Symmetry code
C5-H5A ··· π(C19≡C20)	0.96	2.71	3.365(9)	152(2)	x, 1-y, -1/2+z
		center…center			Symmetry code
π(Cg1)…π(C27≡C28)		3.233(1)			-x, 1-y, 1-z
		2			
D-H ··· *A*	*D*-H	H ··· *A*	*D* ··· *A*	*D*-H ··· *A*	Symmetry code
C1-H1A ··· π(C19≡C20)	0.96	2.48	3.366(9)	149(2)	-x, 1-y, 1+z
		center…center			Symmetry code
π(Cg1)…π(C27≡C28)		3.256(1)			2-x, 1-y, 1-z
		5			
D-H ··· *A*	*D*-H	H ··· *A*	*D* ··· *A*	*D*-H ··· *A*	Symmetry code
C42-H42 ··· Cl1’	0.95	2.89	3.820(3)	166(1)	-x, 1+y, 1/2-z
		center…center			Symmetry code
π(Cg1)…π(C35≡C36)		3.304(1)			-x, 2-y, -z
		6			
D-H ··· *A*	*D*-H	H ··· *A*	*D* ··· *A*	*D*-H ··· *A*	Symmetry code
C21-H21A ··· π(C8≡C9)	0.96	2.78	3.731(3)	171(2)	x, 1-y, -1/2+z
		center…center			Symmetry code
π(Cg2)…π(C35≡C36)		3.303(1)			1-x, 1-y, 1-z

Cg1 is the pyridine ring containing N1 atom, Cg2 is the pyridine ring containing N2 atom.

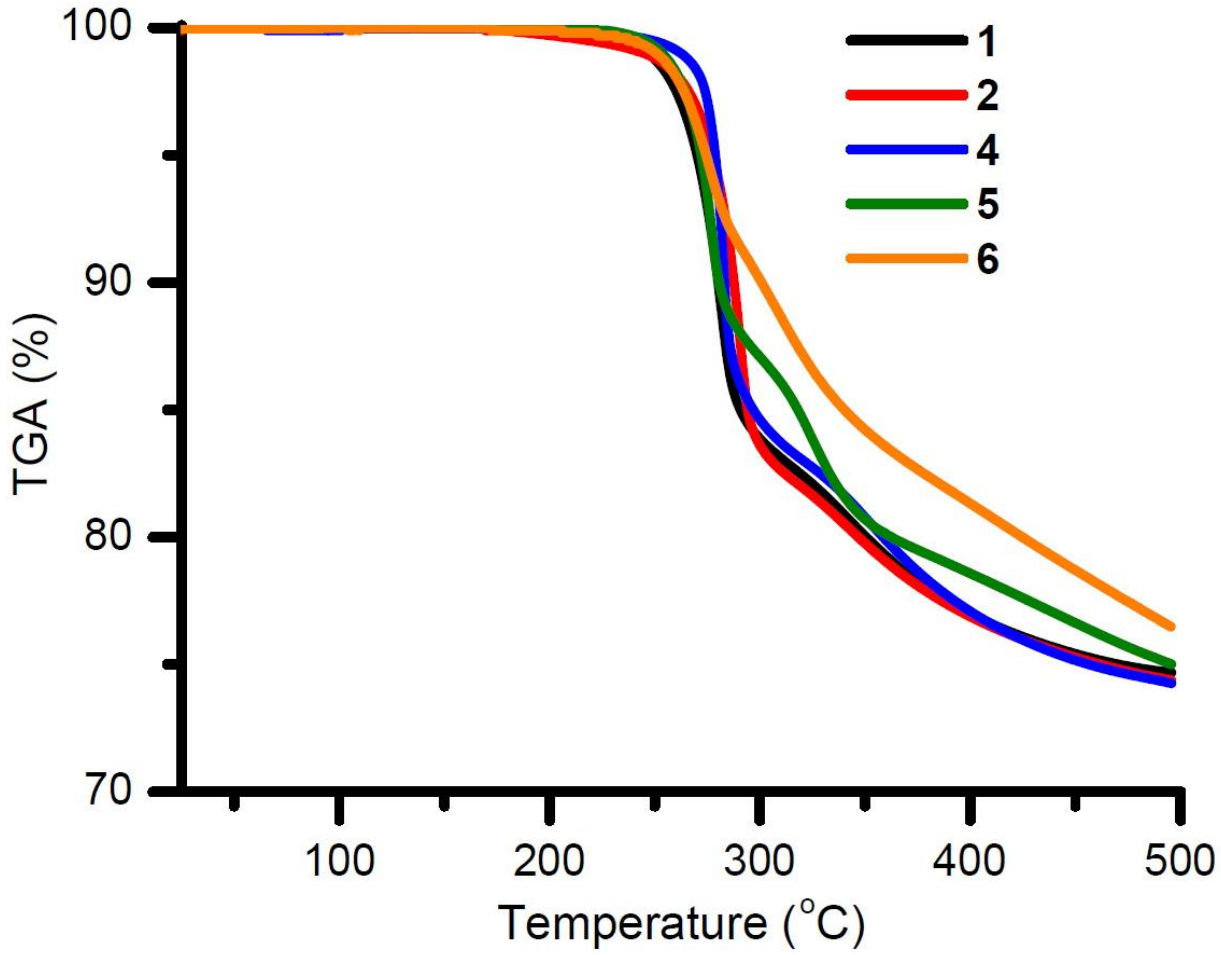

Figure S1. Thermogravimetric analysis curves of complexes **1**, **2**, **4**, **5** and **6** after recrystallized from CH_2Cl_2.

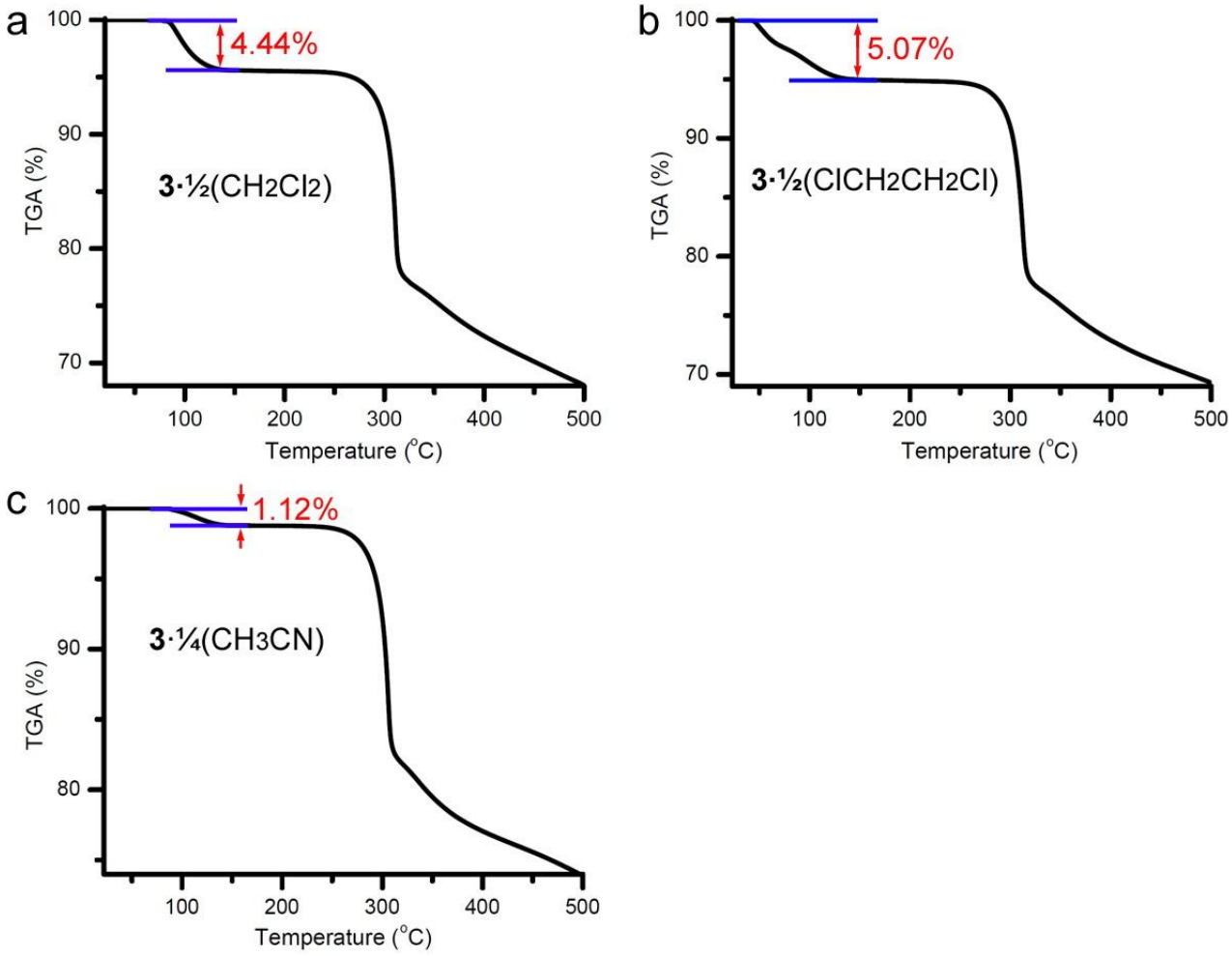

Figure S2. Thermogravimetric analysis curves of complex **3** after recrystallized from CH_2Cl_2, $ClCH_2CH_2Cl$ and CH_3CN.

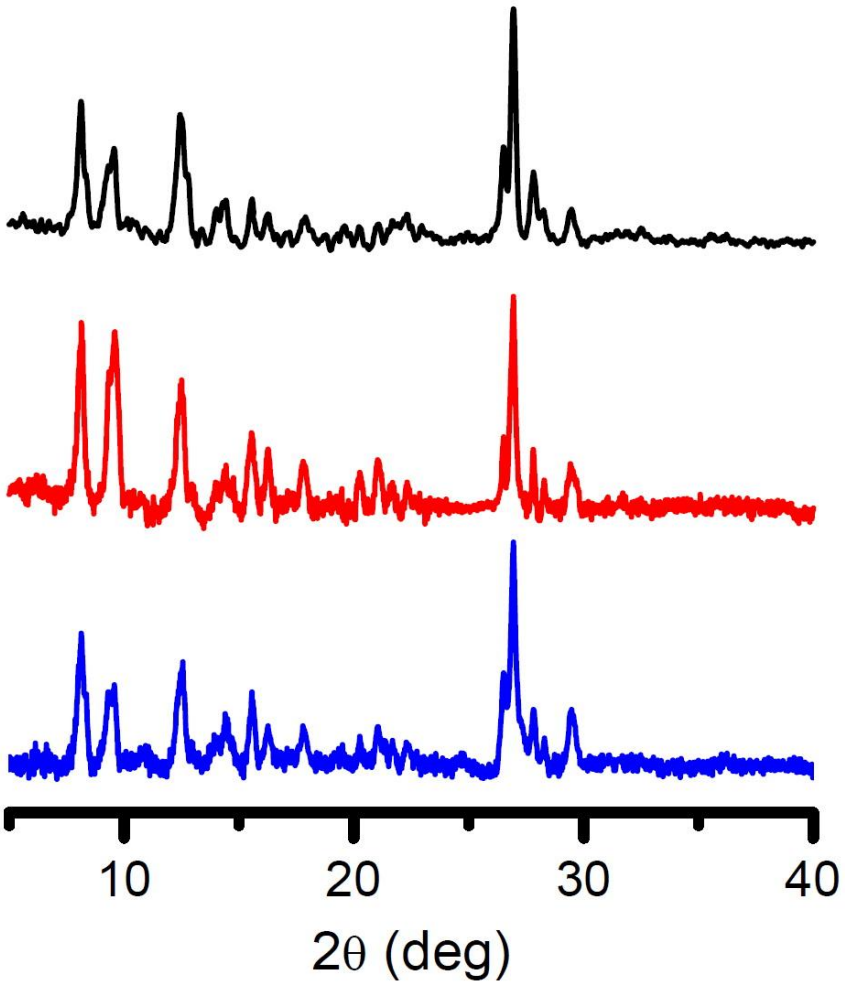

Figure S3. The PXRD patterns of **3** after recrystallized from CH_2Cl_2 (black line), $ClCH_2CH_2Cl$ (red line) and CH_3CN (blue line).

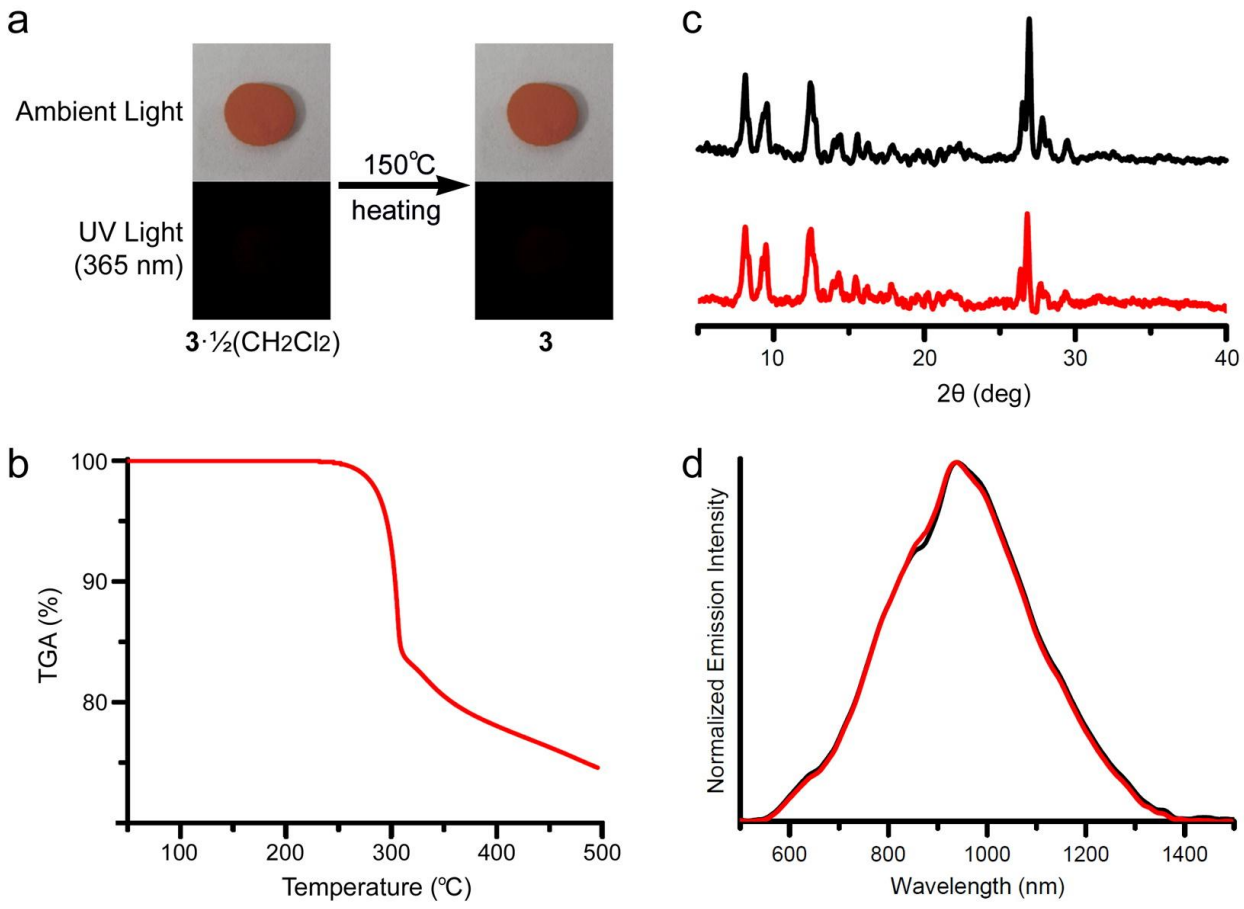

Figure S4. (a) Photographic images under ambient light and UV light irradiation (λ_{ex} = 365 nm) of **3** ½(CH_2Cl_2) before and after heating at 150 ℃. (b) Thermogravimetric analysis curves of **3** ½(CH_2Cl_2) after heating at 150 ℃. (c) PXRD patterns and (d) emission spectra of **3** ½(CH_2Cl_2) before (black line) and after (red line) heating at 150 ℃.

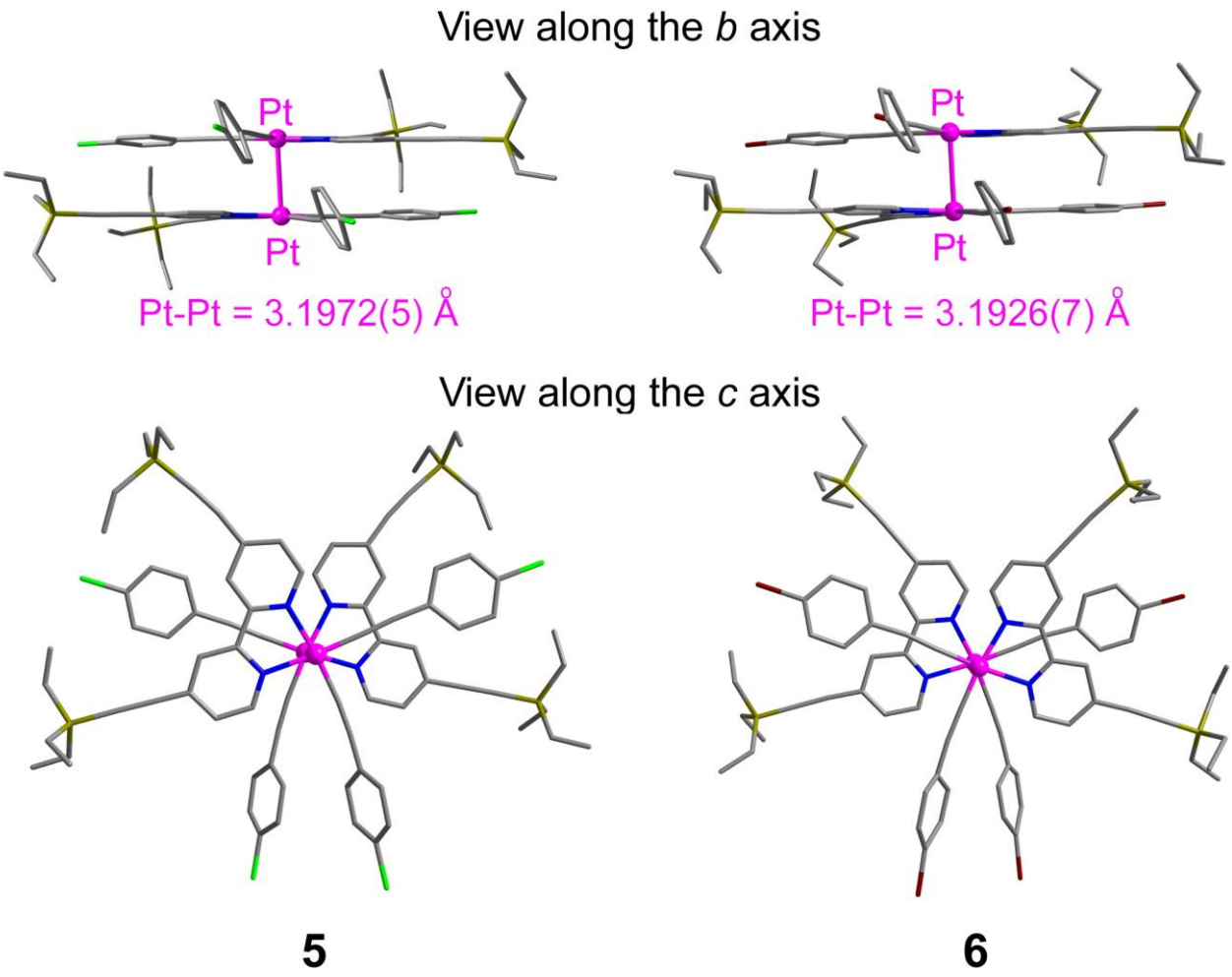

Figure S5. The dimer structure of complexes **5** and **6**. The disordered atoms and H atoms are deleted for clarity.

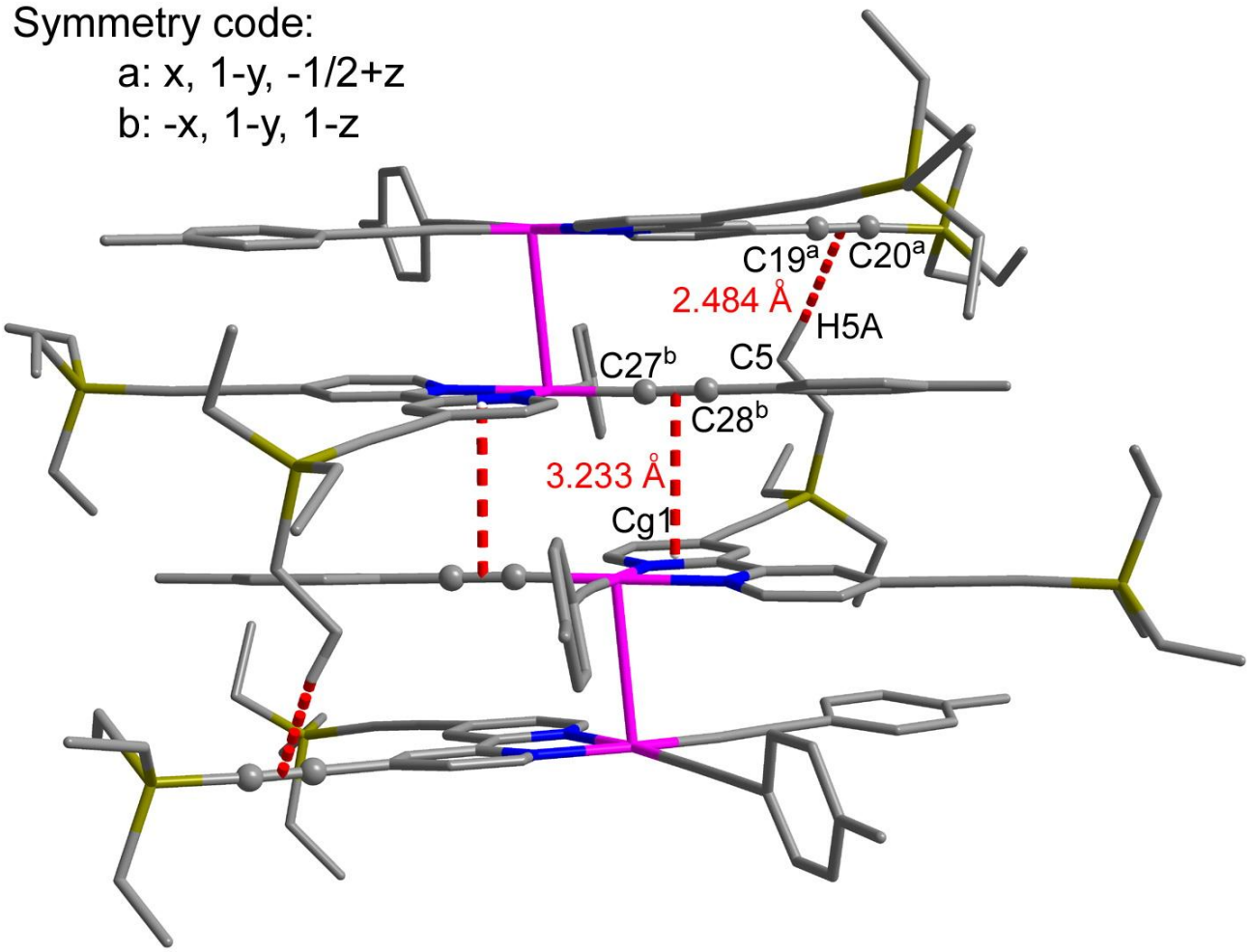

Figure S6. The hydrogen bonding and π-π stacking interactions between adjacent dimers (along *c* axis) of complex **1**.

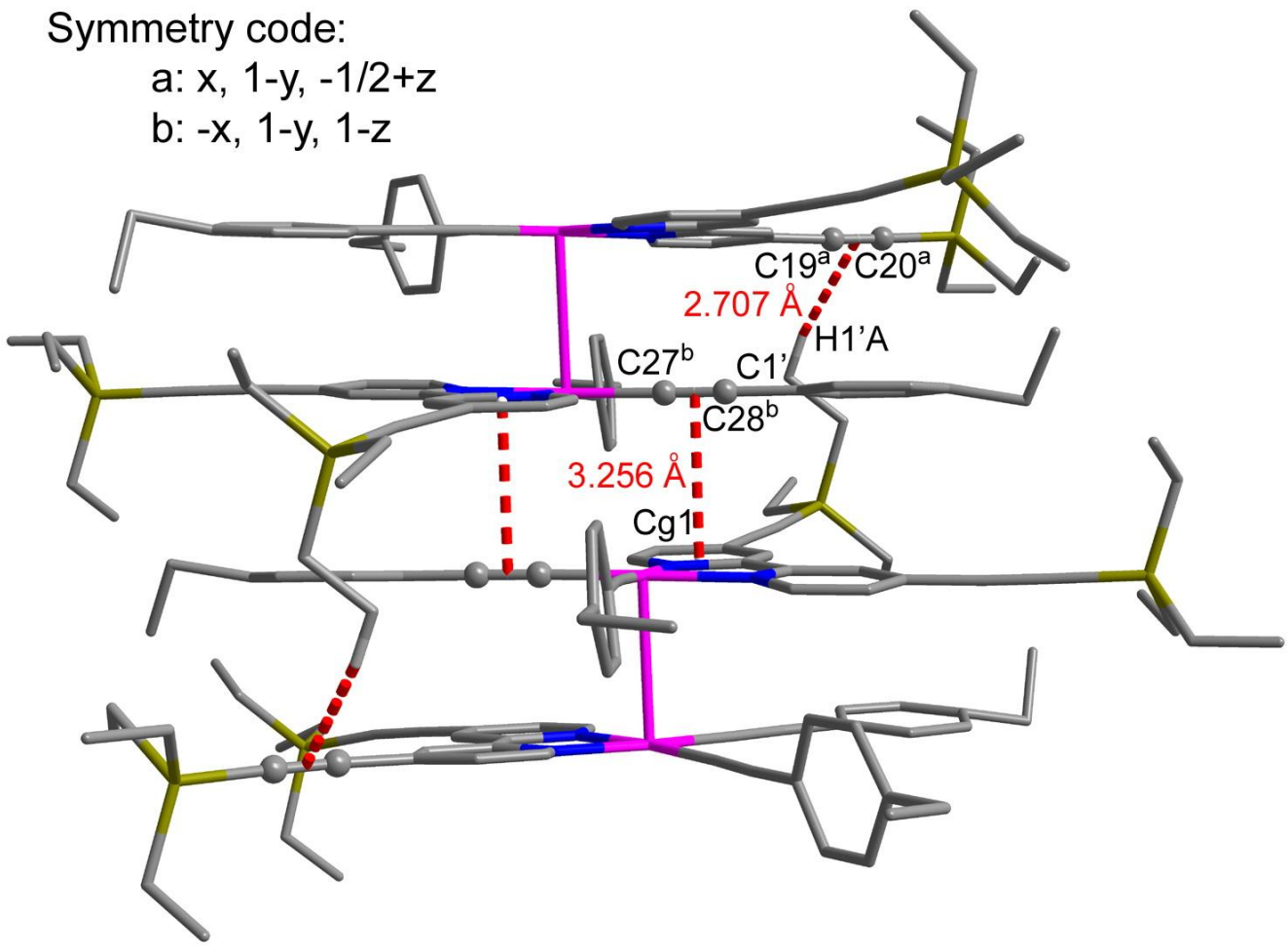

Figure S7. The hydrogen bonding and π-π stacking interactions between adjacent dimers (along *c* axis) of complex **2**.

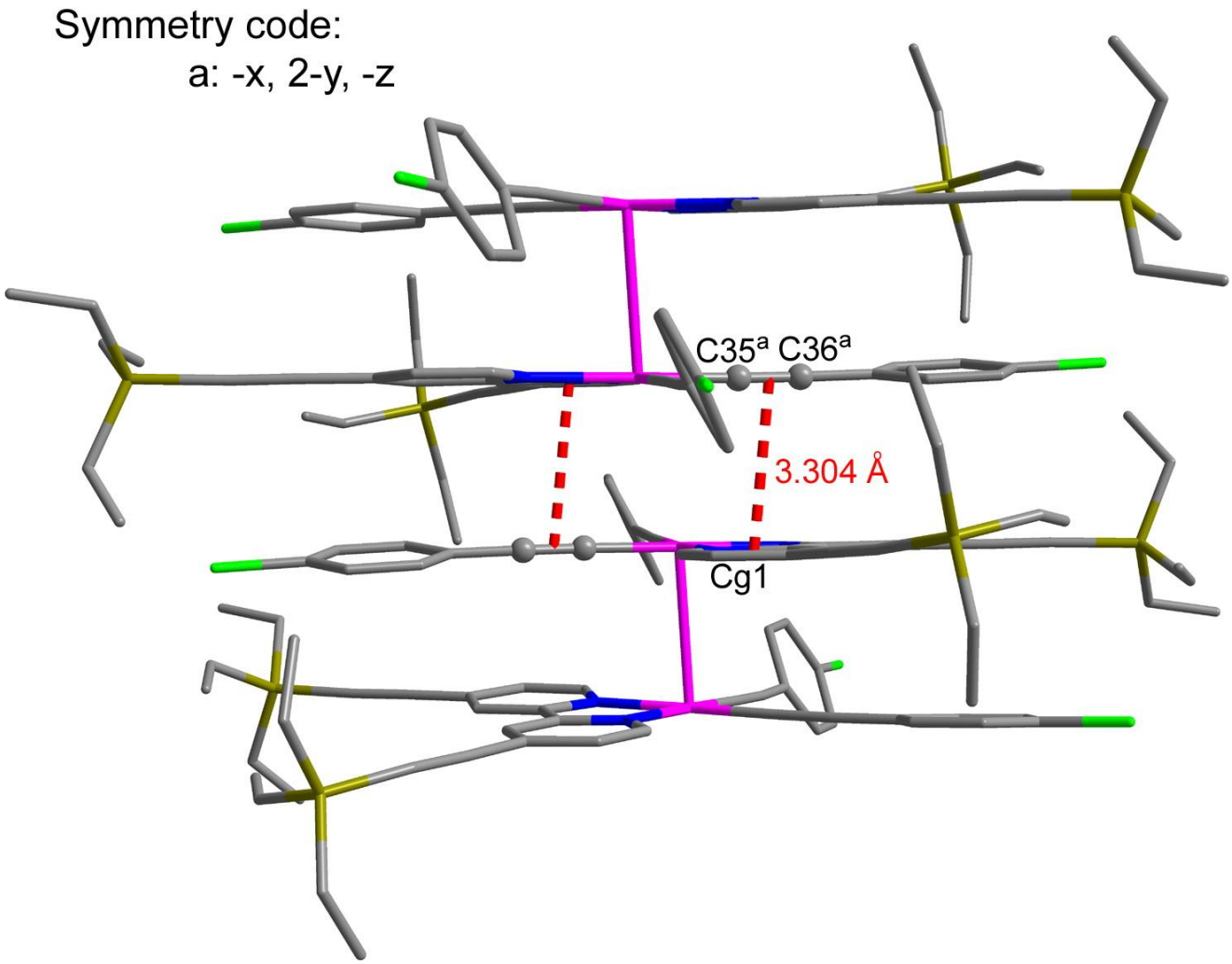

Figure S8. The π-π stacking interactions between adjacent dimers (along *c* axis) of complex **5**.

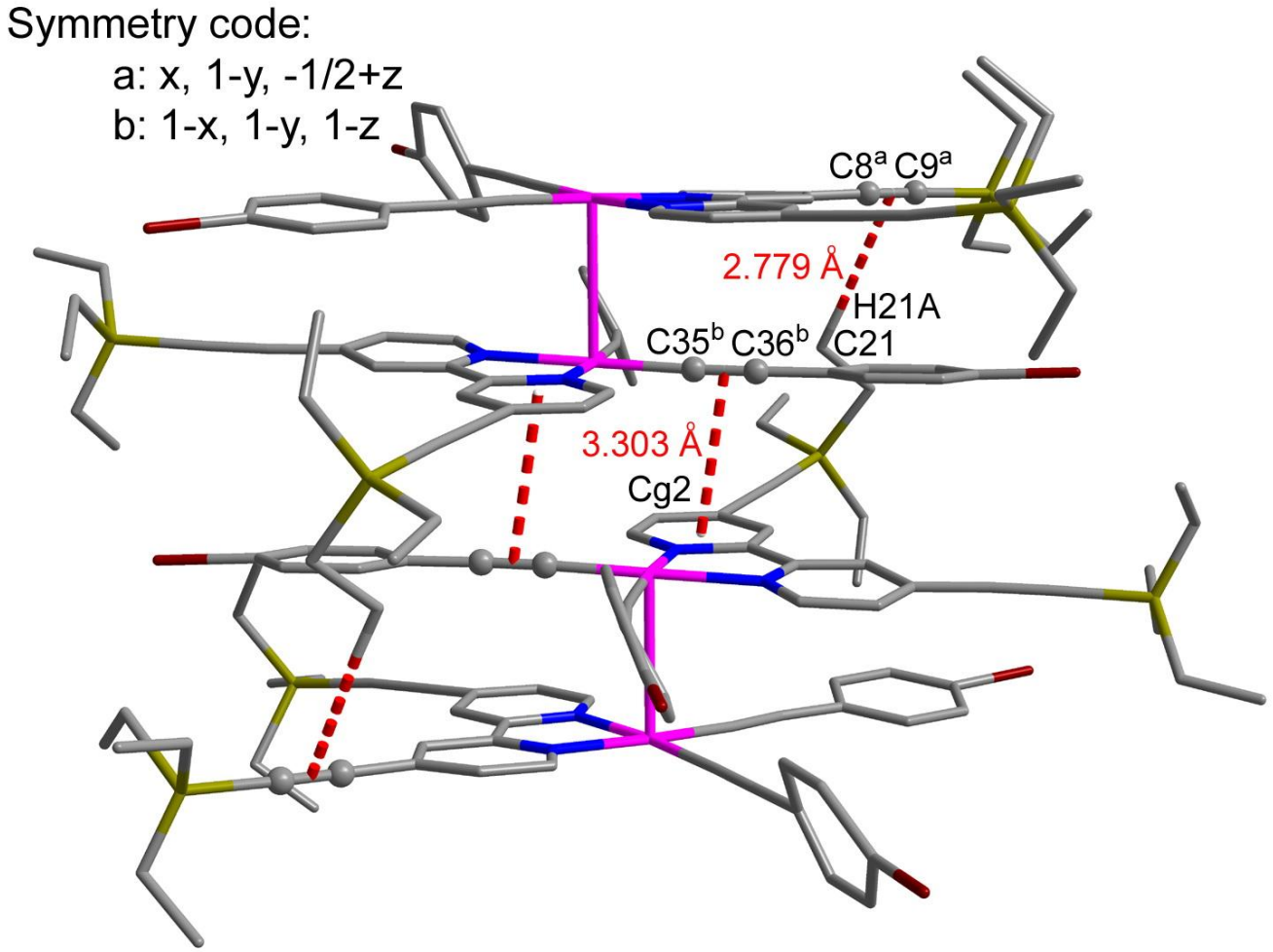

Figure S9. The hydrogen bonding and π-π stacking interactions between adjacent dimers (along *c* axis) of complex **6**.

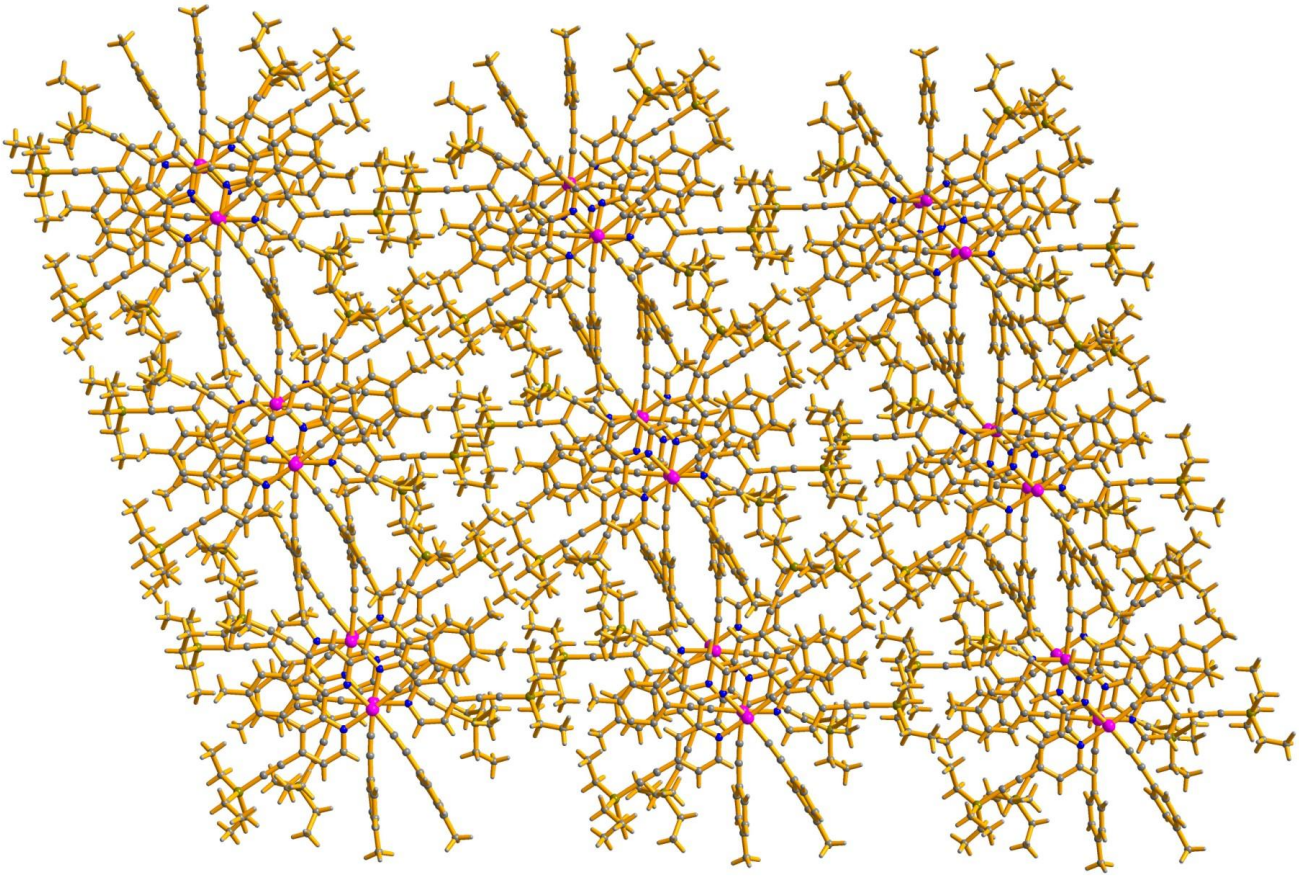

Figure S10. The layer stacking structure of complex **1**.

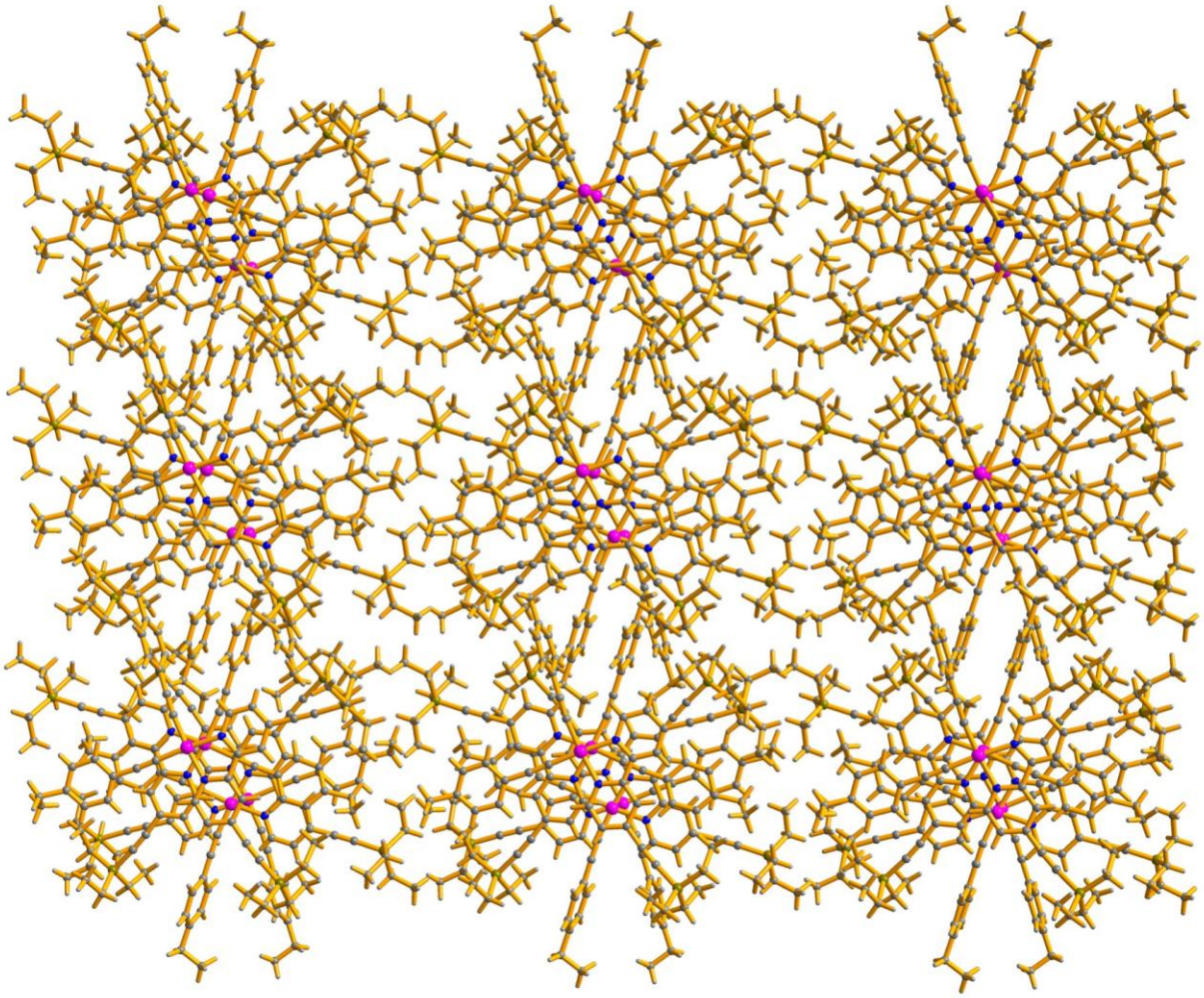

Figure S11. The layer stacking structure of complex **2**.

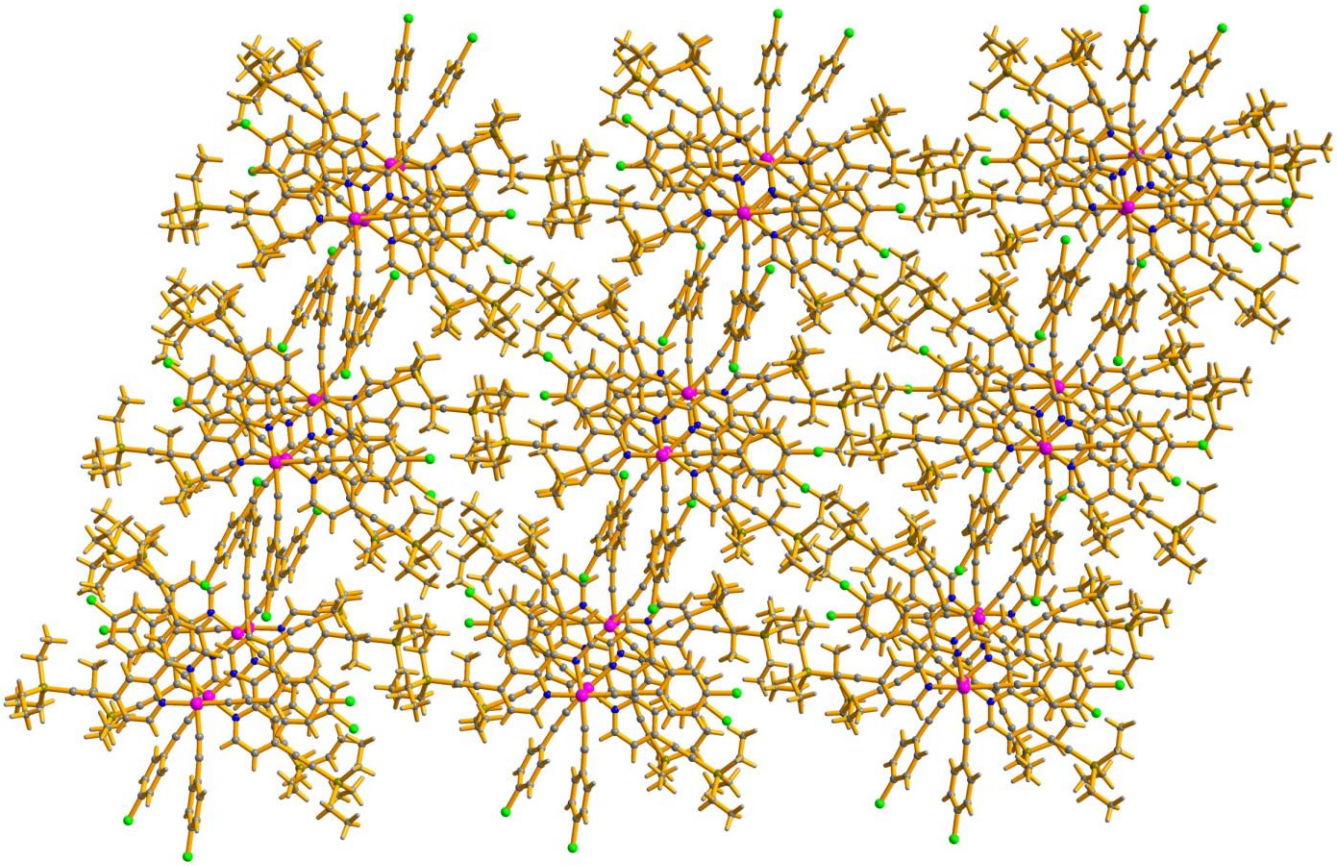

Figure S12. The layer stacking structure of complex **5**.

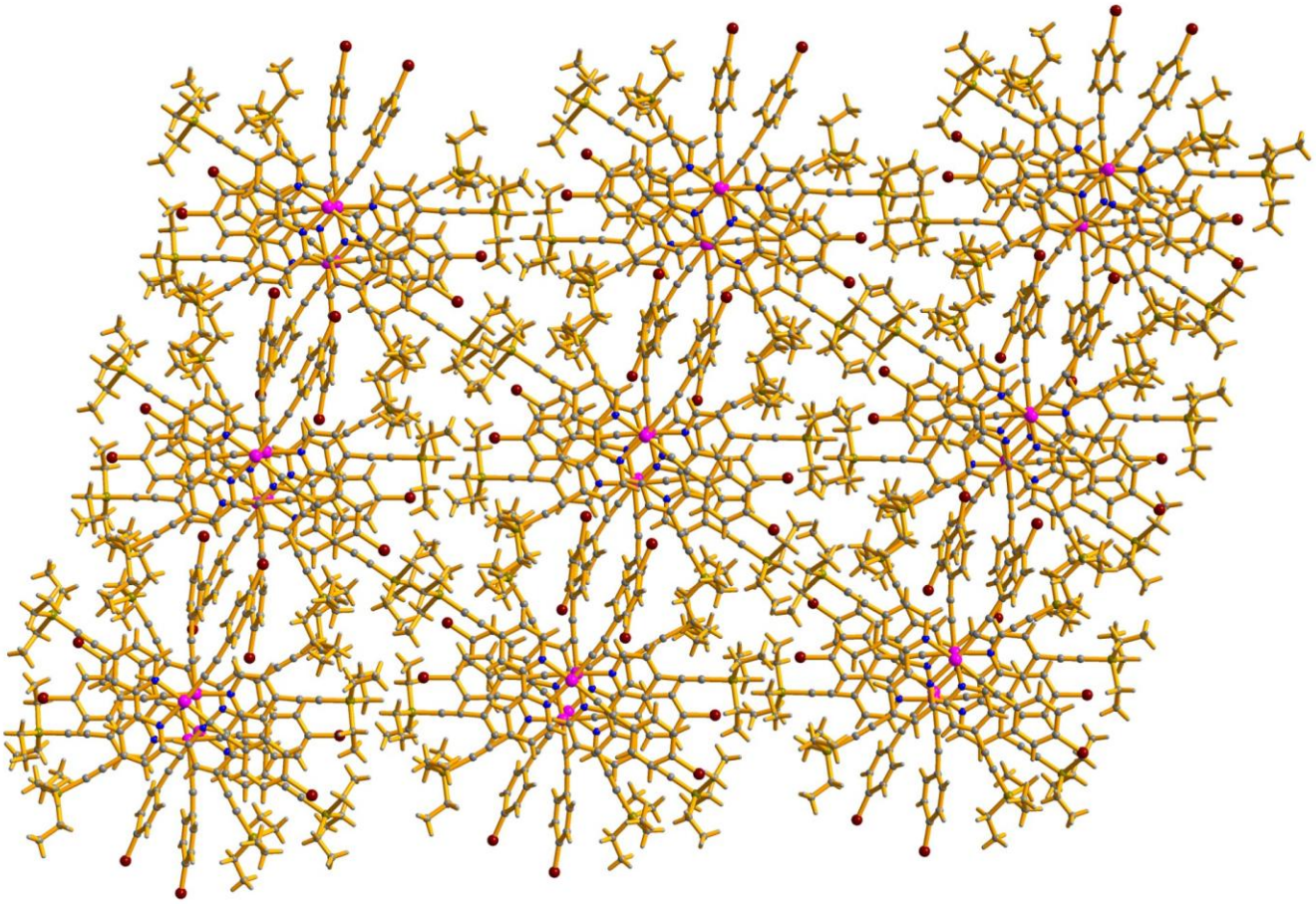

Figure S13. The layer stacking structure of complex **6**.

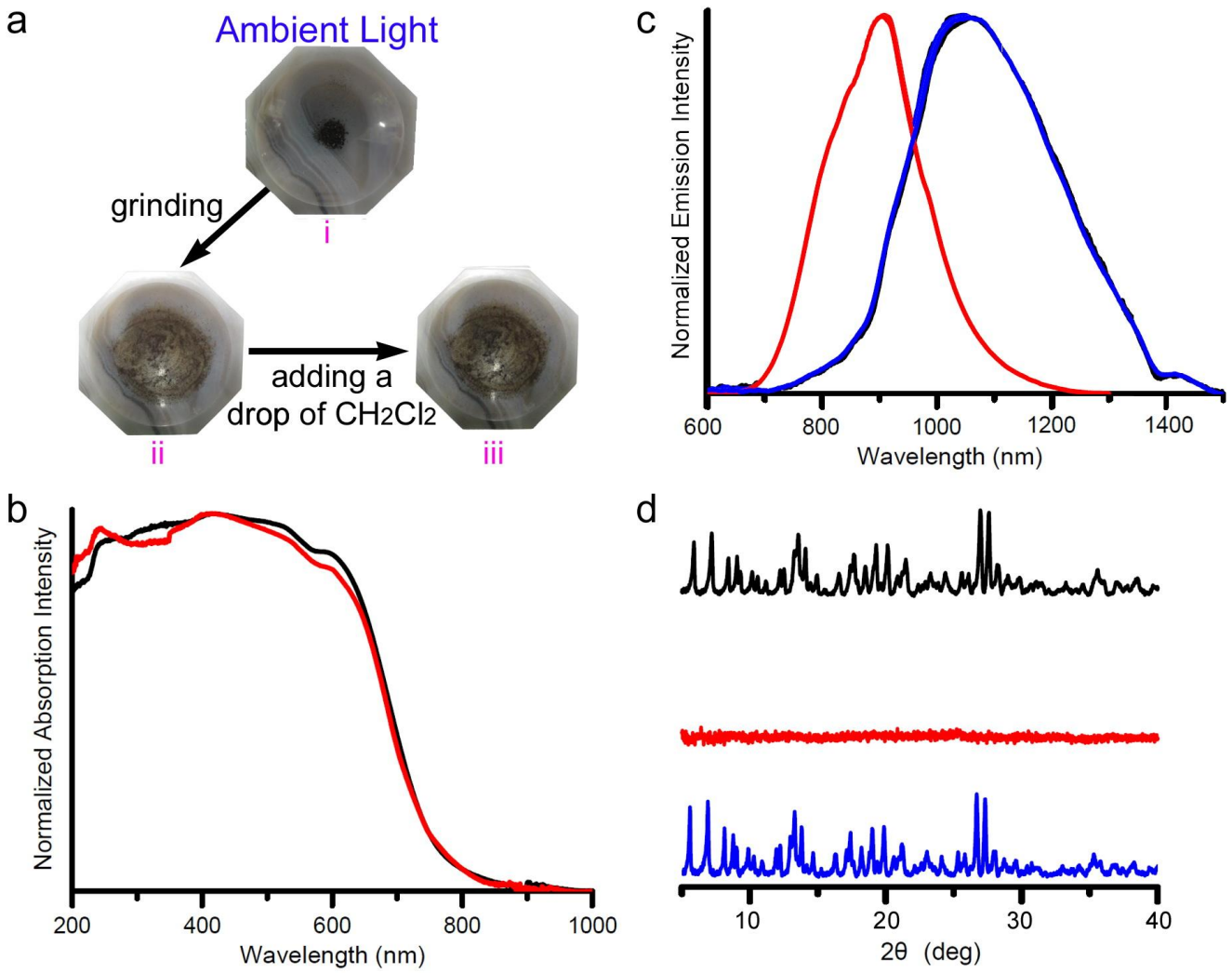

Figure S14. The reversible mechanoluminescence of complex **2**. (a) Photographic images of samples [(i) unground sample, (ii) ground sample, (iii) ground sample with a drop of CH_2Cl_2 added] under ambient light irradiation during the reversible process. (b) Absorption spectra, (c) emission spectra and (d) PXRD patterns of unground sample (black line), ground sample (red line), and ground sample with a drop of CH_2Cl_2 added (blue line).

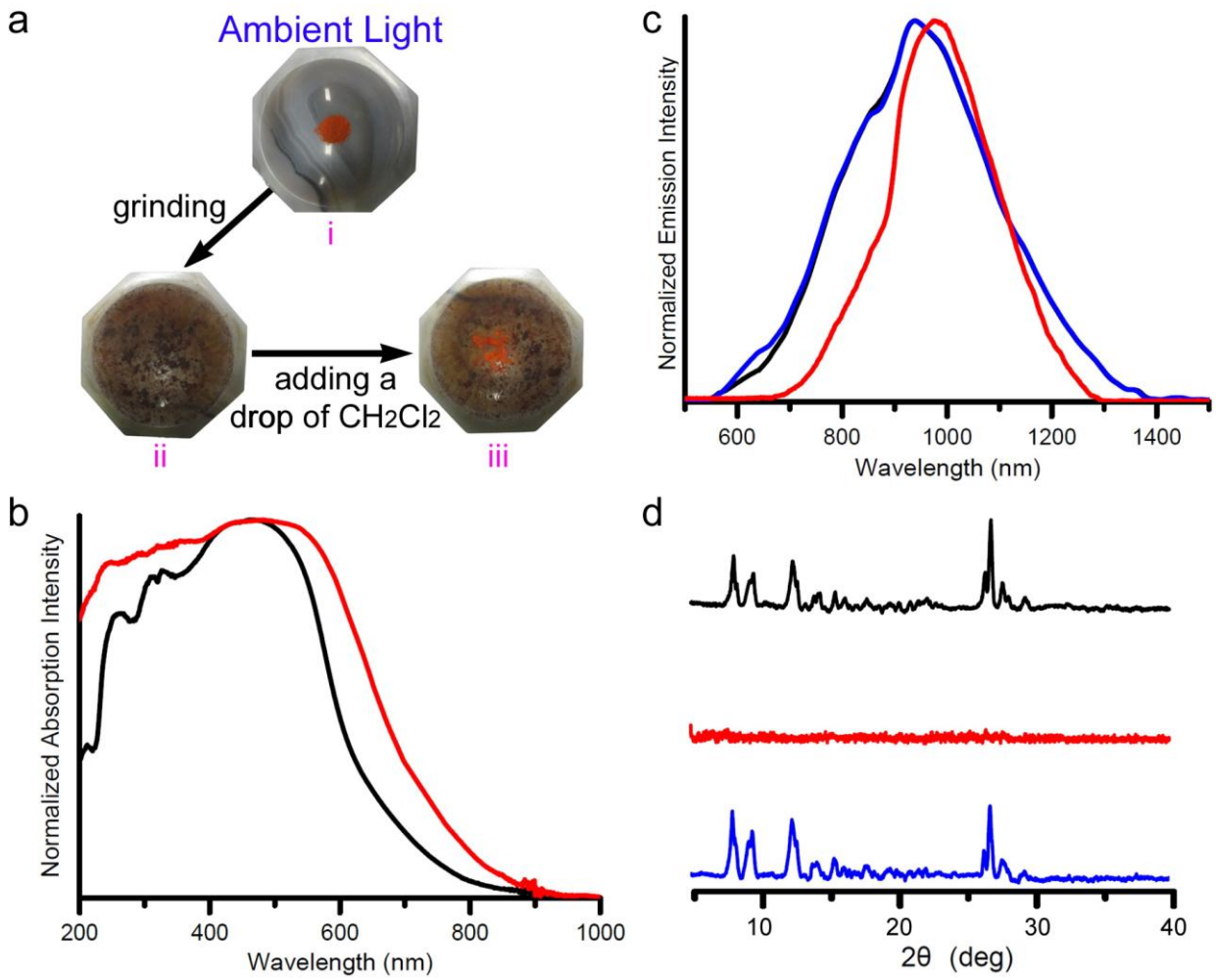

Figure S15. The reversible mechanoluminescence of complex **3**. (a) Photographic images of samples [(i) unground sample, (ii) ground sample, (iii) ground sample with a drop of CH_2Cl_2 added] under ambient light irradiation during the reversible process. (b) Absorption spectra, (c) emission spectra and (d) PXRD patterns of unground sample (black line), ground sample (red line), and ground sample with a drop of CH_2Cl_2 added (blue line).

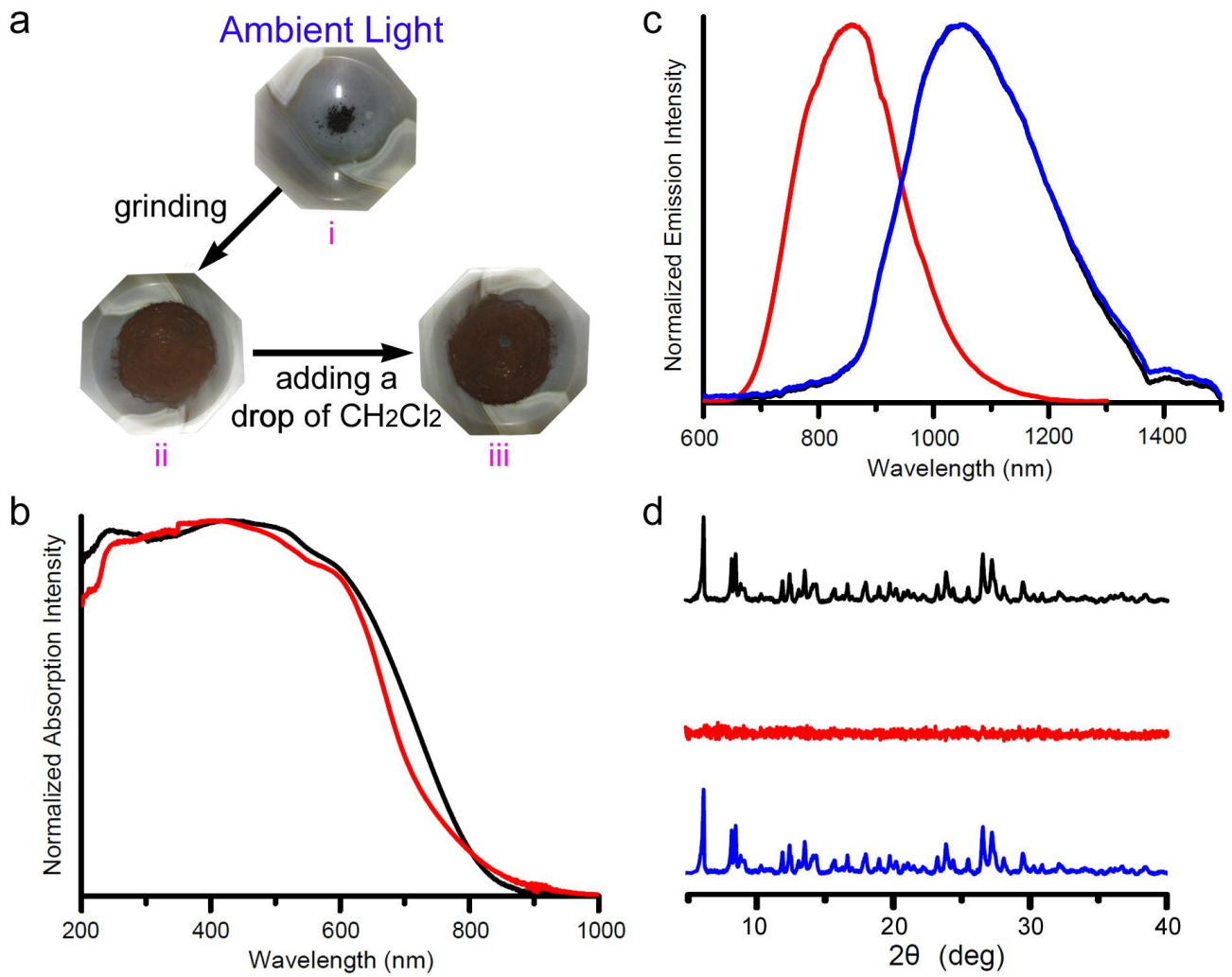

Figure S16. The reversible mechanoluminescence of complex **4**. (a) Photographic images of samples [(i) unground sample, (ii) ground sample, (iii) ground sample with a drop of CH_2Cl_2 added] under ambient light irradiation during the reversible process. (b) Absorption spectra, (c) emission spectra and (d) PXRD patterns of unground sample (black line), ground sample (red line), and ground sample with a drop of CH_2Cl_2 added (blue line).

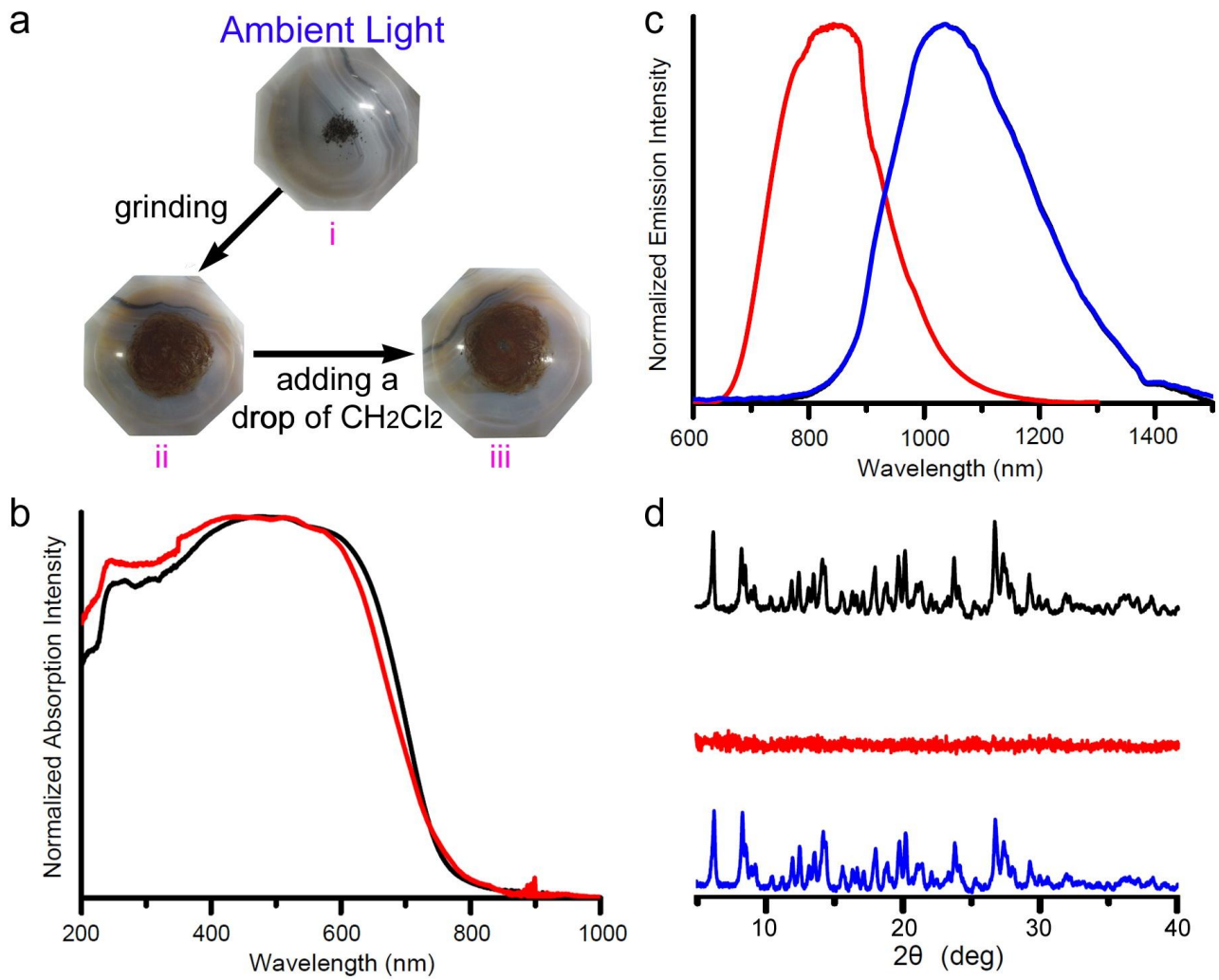

Figure S17. The reversible mechanoluminescence of complex **5**. (a) Photographic images of samples [(i) unground sample, (ii) ground sample, (iii) ground sample with a drop of CH_2Cl_2 added] under ambient light irradiation during the reversible process. (b) Absorption spectra, (c) emission spectra and (d) PXRD patterns of unground sample (black line), ground sample (red line), and ground sample with a drop of CH_2Cl_2 added (blue line).

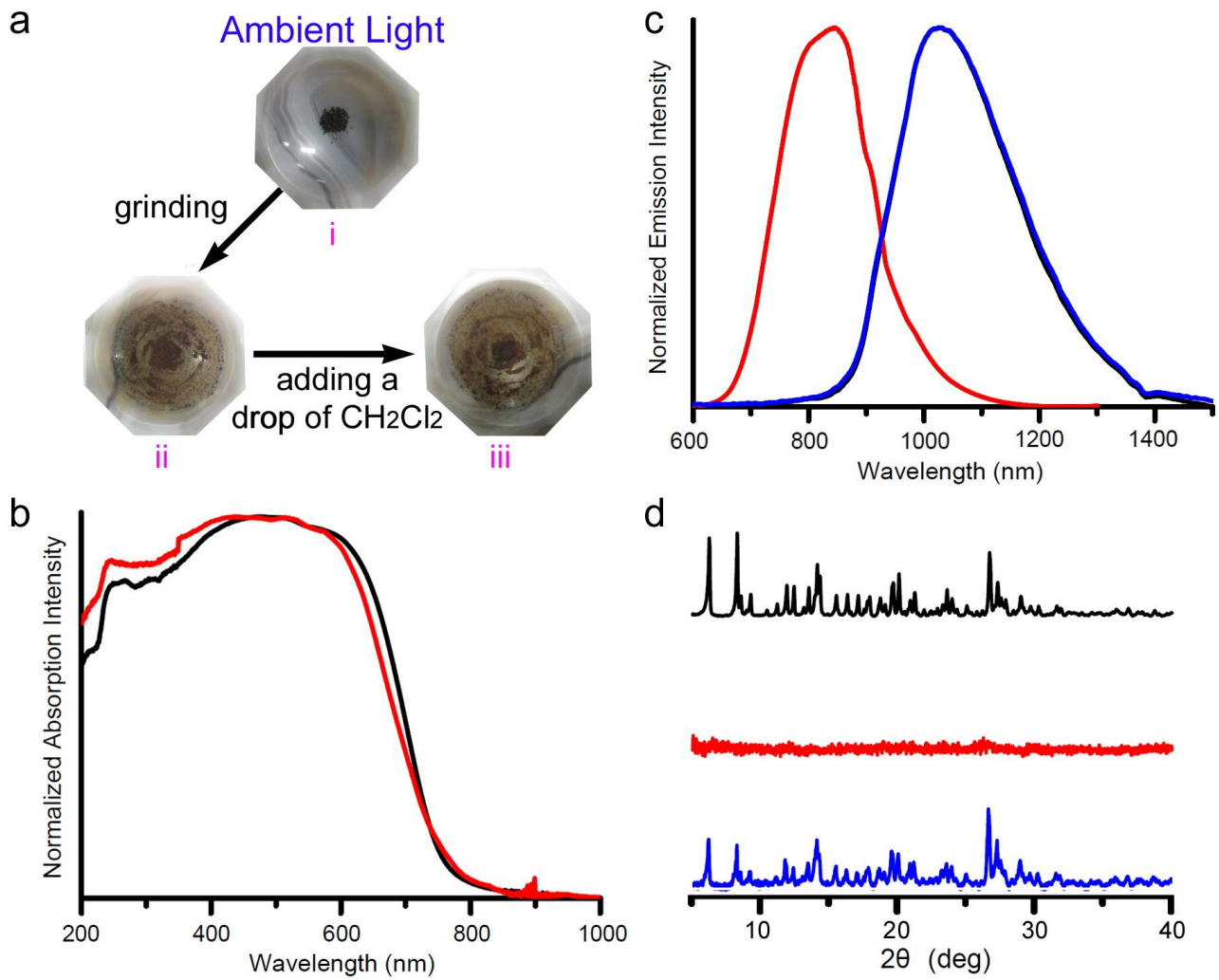

Figure S18. The reversible mechanoluminescence of complex **6**. (a) Photographic images of samples [(i) unground sample, (ii) ground sample, (iii) ground sample with a drop of CH_2Cl_2 added] under ambient light irradiation during the reversible process. (b) Absorption spectra, (c) emission spectra and (d) PXRD patterns of unground sample (black line), ground sample (red line), and ground sample with a drop of CH_2Cl_2 added (blue line).

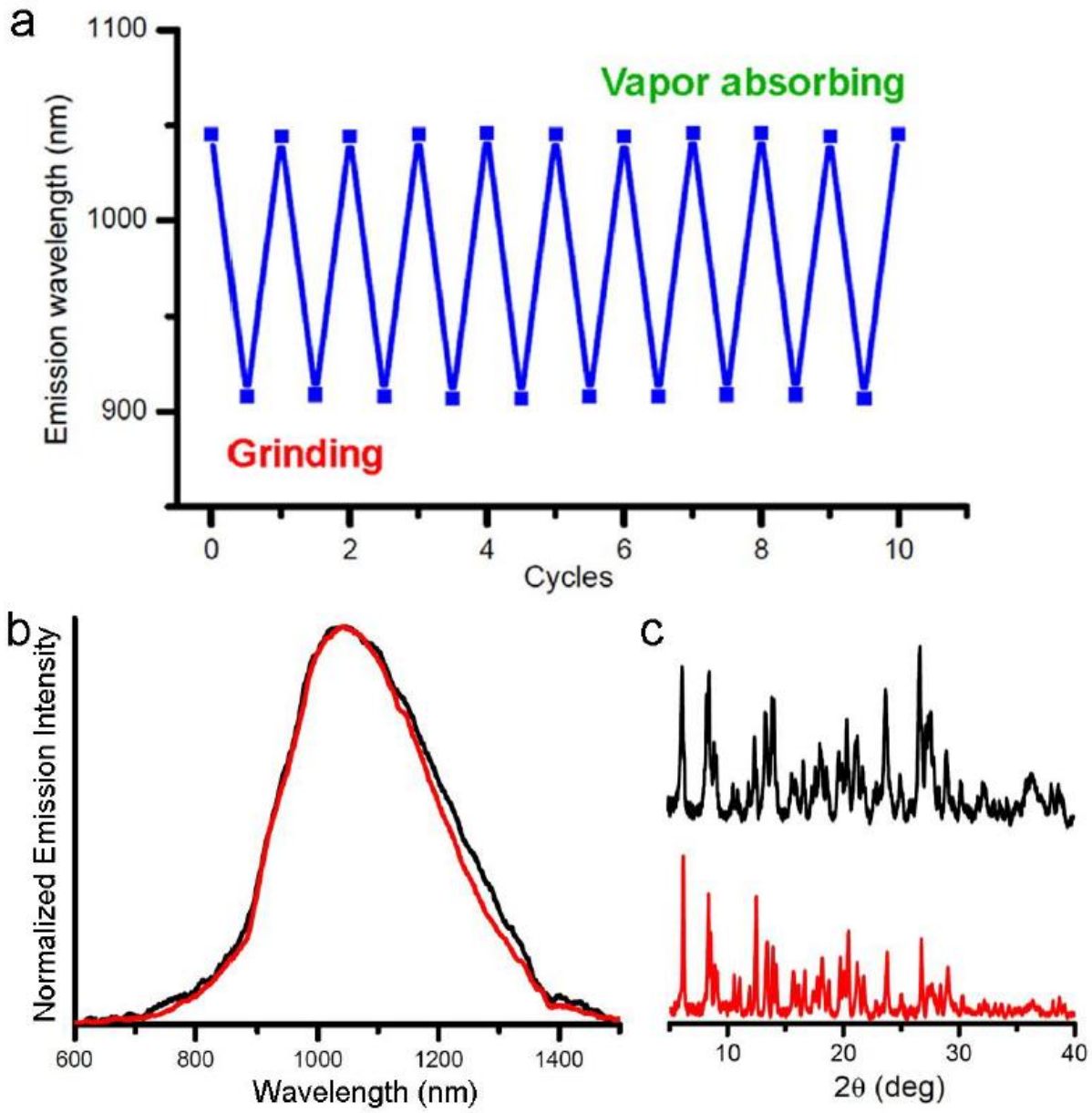

Figure S19. (a) Plot of emission wavelength changes during 10-cycles of grinding/vapor absorbing process of **1**. (b) Luminescence spectra and (c) PXRD pattern of **1** before and after 10-cycles of grinding/vapor absorbing process.

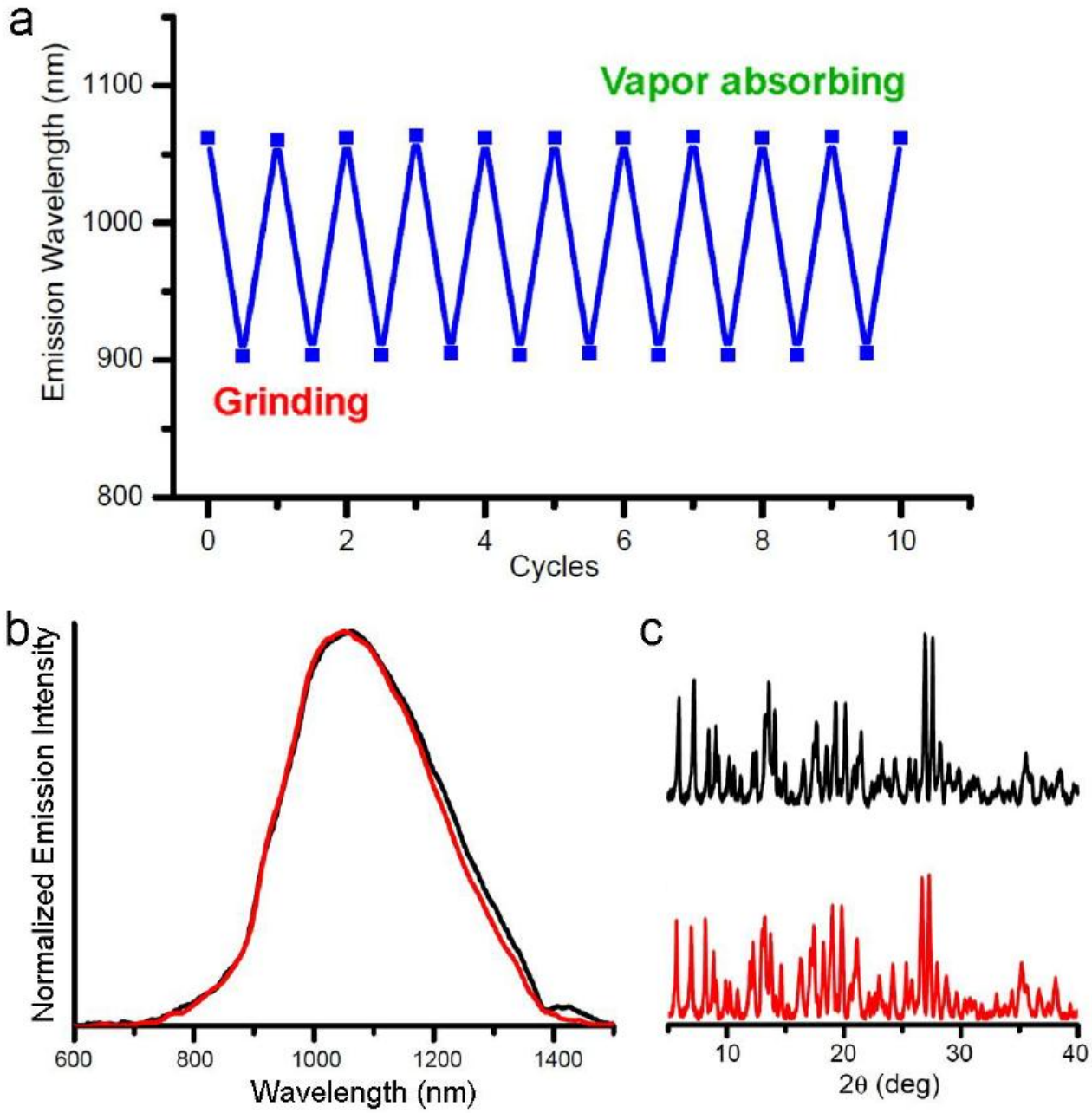

Figure S20. (a) Plot of emission wavelength changes during 10-cycles of grinding/vapor absorbing process of **2**. (b) Luminescence spectra and (c) PXRD pattern of **2** before and after 10-cycles of grinding/vapor absorbing process.

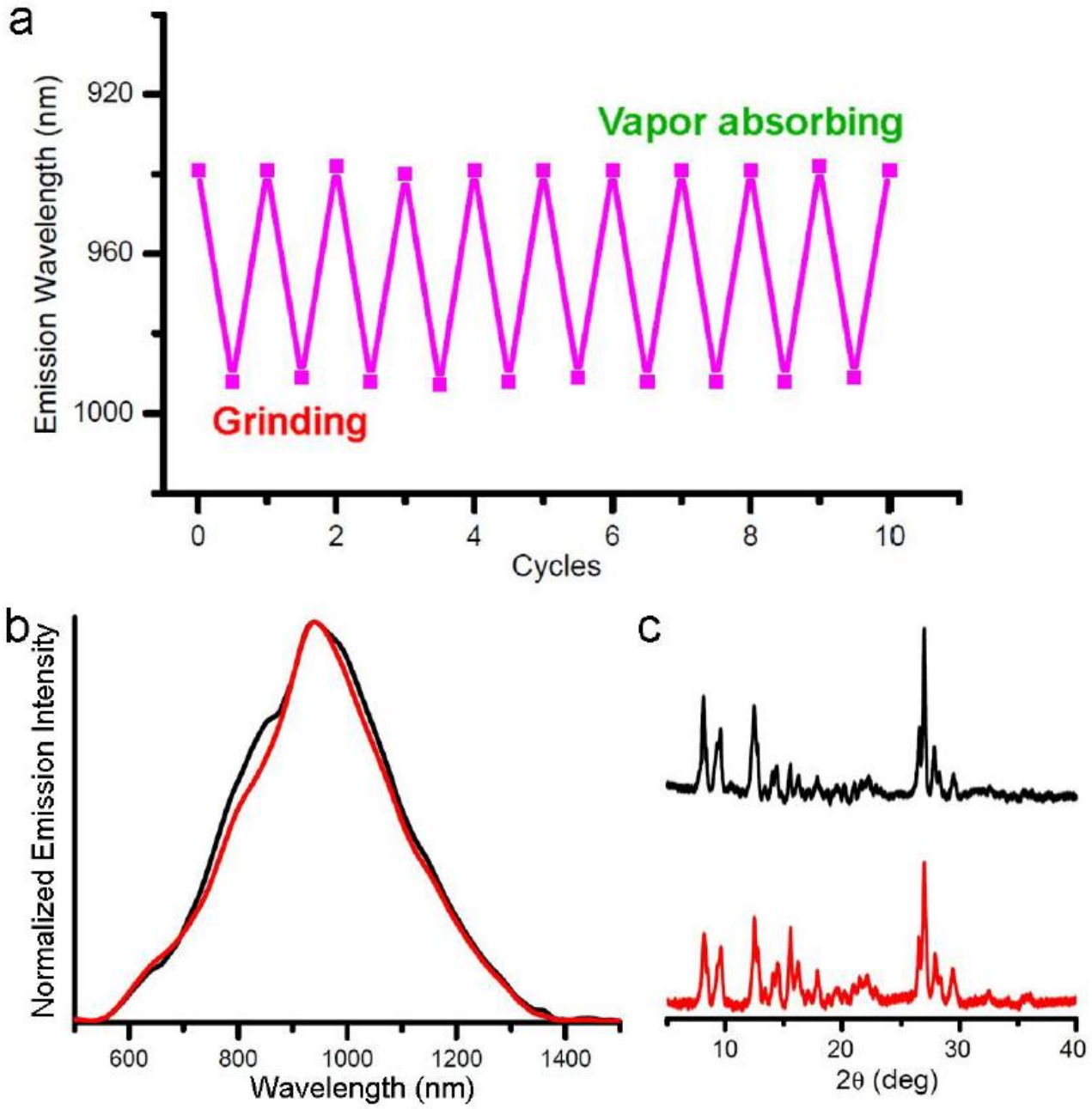

Figure S21. (a) Plot of emission wavelength changes during 10-cycles of grinding/vapor absorbing process of **3**. (b) Luminescence spectra and (c) PXRD pattern of **3** before and after 10-cycles of grinding/vapor absorbing process.

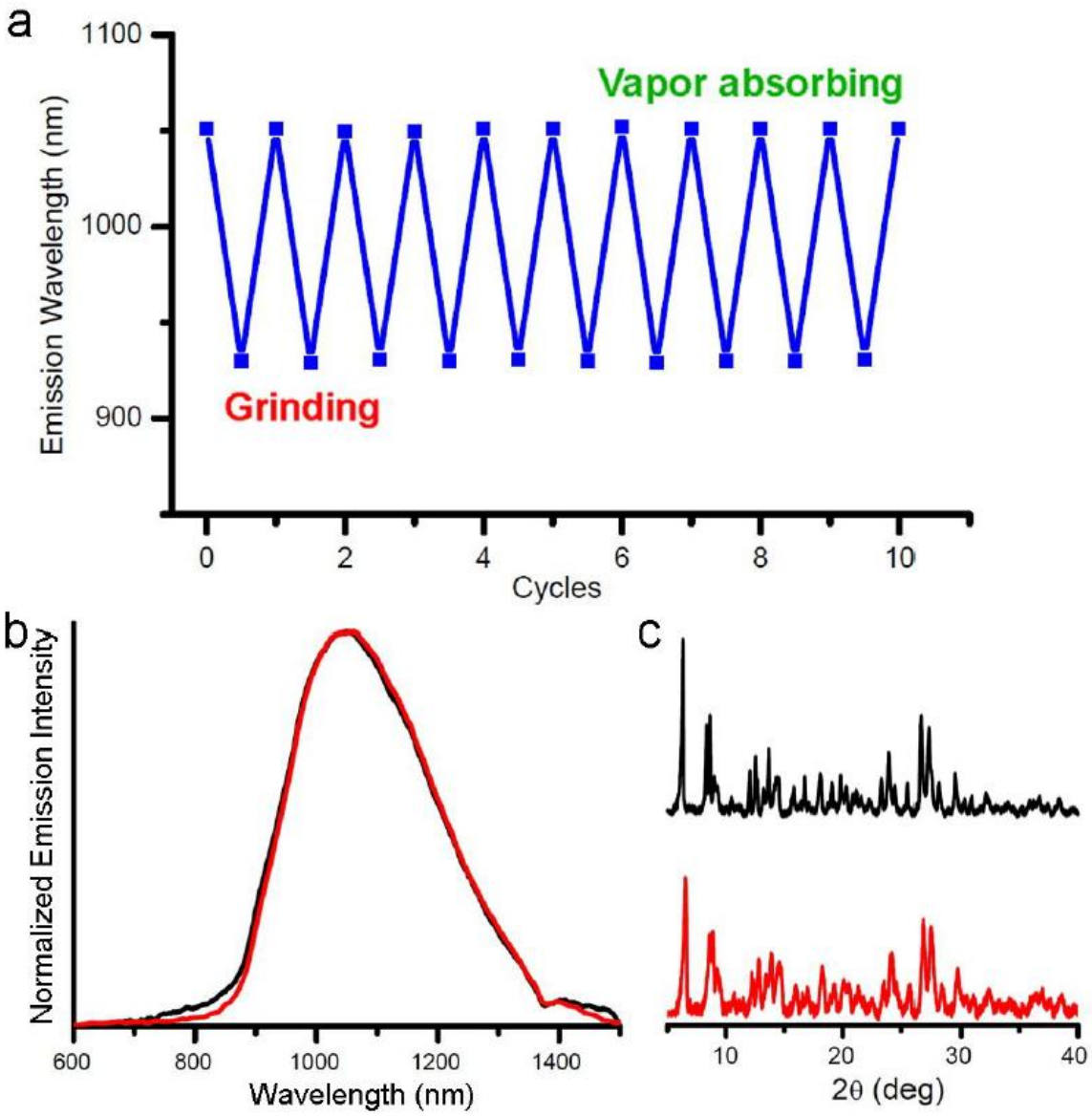

Figure S22. (a) Plot of emission wavelength changes during 10-cycles of grinding/vapor absorbing process of **4**. (b) Luminescence spectra and (c) PXRD pattern of **4** before and after 10-cycles of grinding/vapor absorbing process.

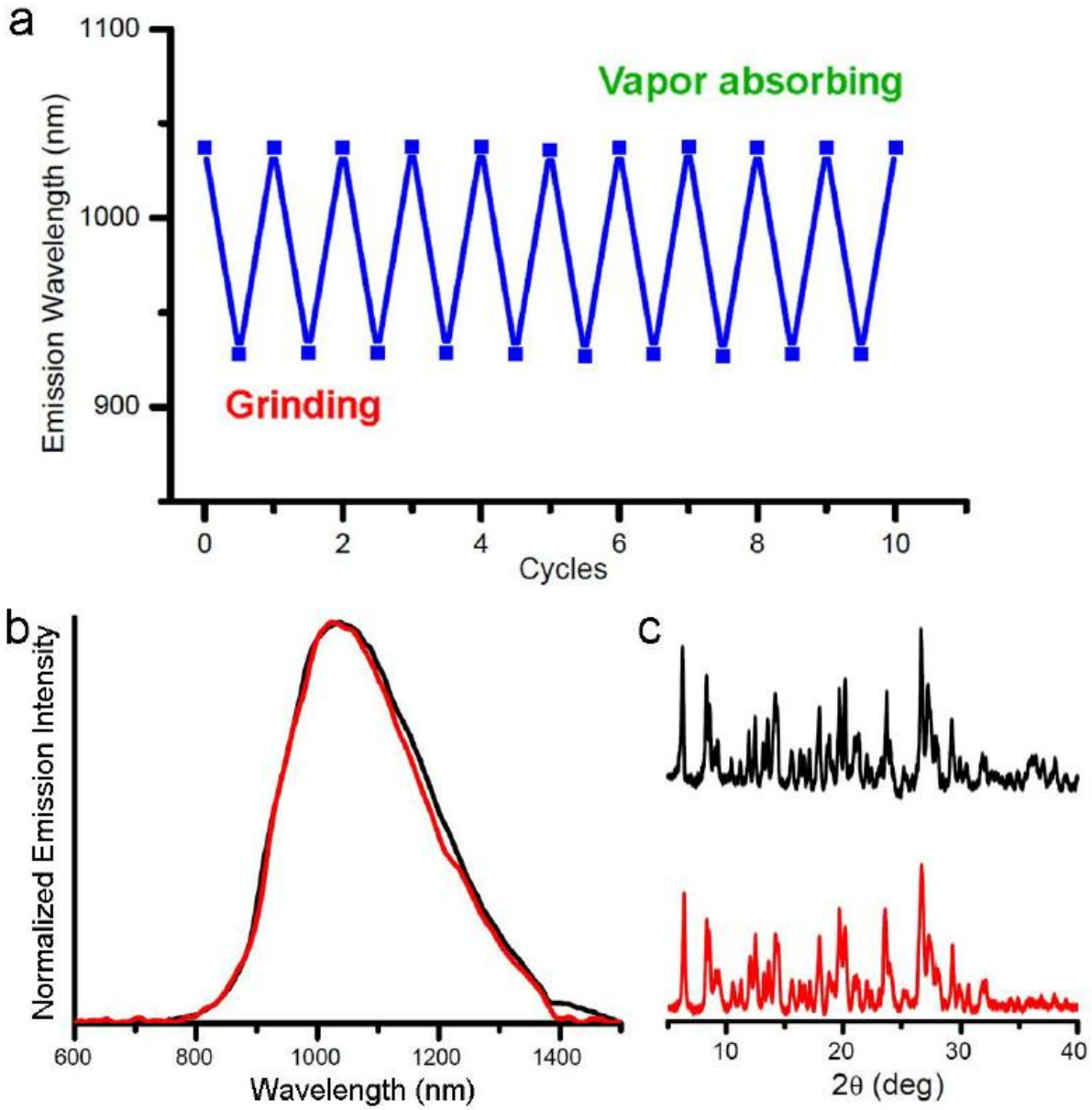

Figure S23. (a) Plot of emission wavelength changes during 10-cycles of grinding/vapor absorbing process of **5**. (b) Luminescence spectra and (c) PXRD pattern of **5** before and after 10-cycles of grinding/vapor absorbing process.

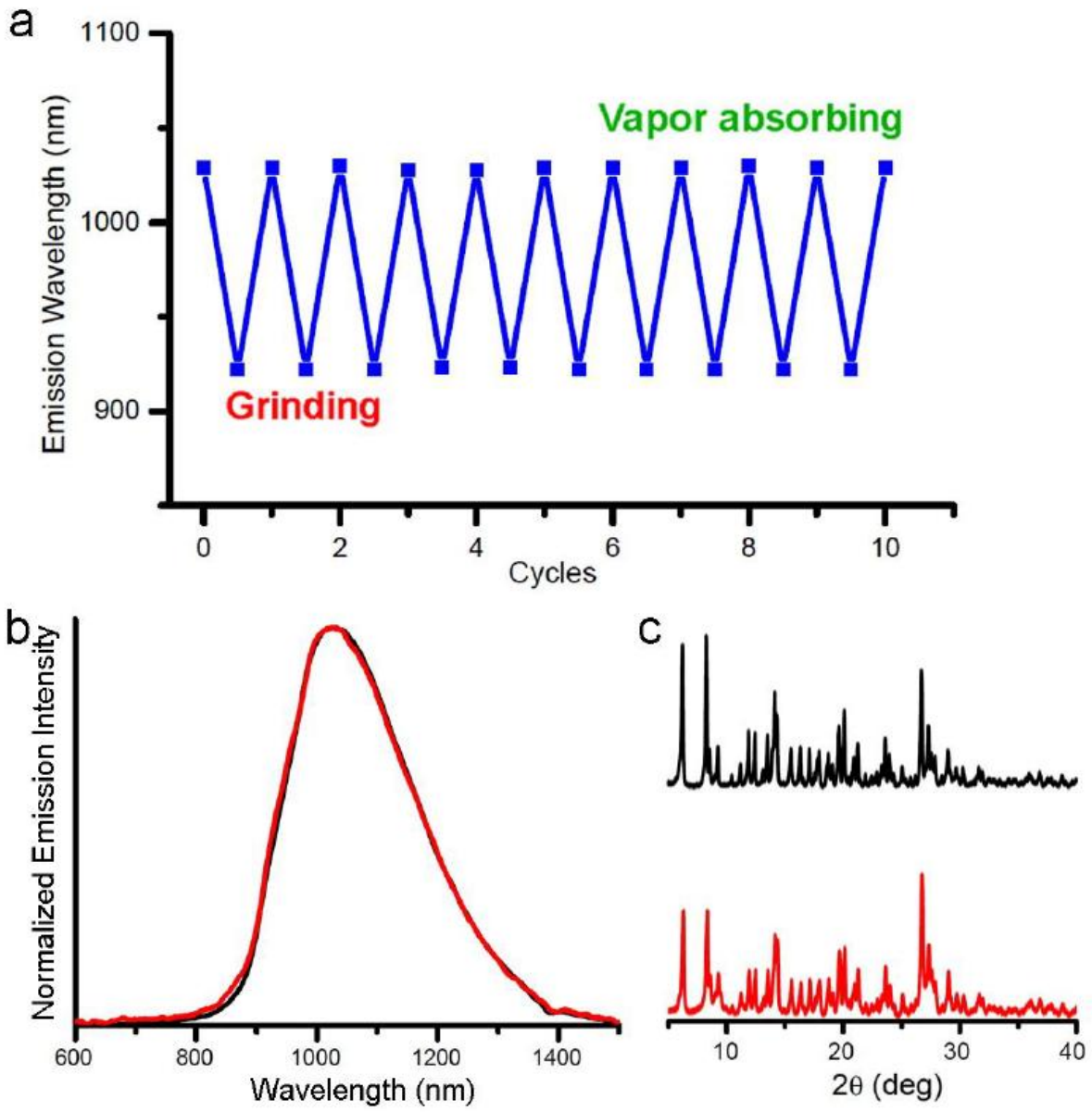

Figure S24. (a) Plot of emission wavelength changes during 10-cycles of grinding/vapor absorbing process of **6**. (b) Luminescence spectra and (c) PXRD pattern of **6** before and after 10-cycles of grinding/vapor absorbing process.